Journal of Power Sources 256 (2014) 88–95

Contents lists available at ScienceDirect

Journal of Power Sources

journal homepage: www.elsevier.com/locate/jpowsour

Development of carbon nanotube and graphite filled polyphenylene sulfide based bipolar plates for all-vanadium redox flow batteries

Burak Caglar [a,*], Peter Fischer [a], Pertti Kauranen [c], Mikko Karttunen [c], Peter Elsner [b]

[a] Fraunhofer Institute for Chemical Technology (ICT), Applied Electrochemistry Department, Joseph-von-Fraunhofer Str. 7, 76327 Pfinztal, Germany
[b] Fraunhofer Institute for Chemical Technology (ICT), Polymer Engineering Department, Joseph-von-Fraunhofer Str. 7, 76327 Pfinztal, Germany
[c] VTT Technical Research Centre of Finland, P.O. Box 1300, 33101 Tampere, Finland

HIGHLIGHTS

- Injection molded bipolar plates are evaluated for all-vanadium redox flow battery.
- Carbon nanotubes possess promising features as secondary conductive filler.
- Titanate coupling agent increases the electrical conductivity of bipolar plates.
- Developed bipolar plates show favorable surface structures for redox reactions.

ARTICLE INFO

Article history:
Received 18 November 2013
Received in revised form
23 December 2013
Accepted 16 January 2014
Available online 23 January 2014

Keywords:
Bipolar plate
Polymer composite
Carbon nanotubes
Vanadium redox flow battery
Corrosion measurements

ABSTRACT

In this study, synthetic graphite and carbon nanotube (CNT) filled polyphenylene sulfide (PPS) based bipolar plates are produced by using co-rotating twin-screw extruder and injection molding. Graphite is the main conductive filler and CNTs are used as bridging filler between graphite particles. To improve the dispersion of the fillers and the flow behavior of the composite, titanate coupling agent (KR-TTS) is used. The concentration effect of CNTs and coupling agent on the properties of bipolar plates are examined. At 72.5 wt.% total conductive filler concentration, by addition of 2.5 wt.% CNT and 3 wt.% KR-TTS; through-plane and in-plane electrical conductivities increase from 1.42 S cm^{-1} to 20 S cm^{-1} and 6.4 S cm^{-1} to 57.3 S cm^{-1} respectively compared to sample without CNTs and additive. Extruder torque value and apparent viscosity of samples decrease significantly with coupling agent and as a result; the flow behavior is positively affected. Flexural strength is improved 15% by addition of 1.25 wt.% CNT. Differential scanning calorimeter (DSC) analysis shows nucleating effect of conductive fillers on PPS matrix. Corrosion measurements, cyclic voltammetry and galvanostatic charge–discharge tests are performed to examine the electrochemical stability and the performance of produced bipolar plates in all-vanadium redox flow battery.

1. Introduction

All-vanadium redox flow battery (VRFB) is a secondary type battery which uses the electrolyte of vanadium (V) element in both half-cells [1]. It was invented almost three decades ago and has gained considerable attention and used in applications such as; uninterruptible power supply, battery for wind turbine generator, load leveling of electrical power stations and remote area power sources due to its highly efficient and reliable energy storage characteristics [2]. In VRFB, on the contrary to conventional batteries, electrolyte is stored in tanks and pumped into the related half-cells. This design gives opportunity to the control of power density and energy density independently. While the higher volume and concentration of the electrolyte are increasing the energy density, power density is dependent on the surface area of the electrode and the reaction rate on the electrode surface [3]. Oxidation and reduction reactions occur on the surface of porous carbon-electrode and the H^+ ion balance between half-cells is controlled by the proton exchange membrane. Produced electrons are transferred to the following cell or out of the battery to complete the circuit by bipolar plates. The anode and cathode reactions of VRFB are as follows and standard electrode potentials are given vs. reversible hydrogen electrode (RHE):

$$\text{Anode}: \quad V^{2+} \leftrightarrow V^{3+} + e^- \quad E^o = -0.26\ \text{V vs. RHE} \tag{1}$$

* Corresponding author. Tel.: +49 721 4640 514; fax: +49 721 4640 318.
E-mail addresses: burak.caglar@ict.fraunhofer.de, burak_caglar1903@yahoo.com (B. Caglar).

0378-7753/$ – see front matter © 2014 Elsevier B.V. All rights reserved.
http://dx.doi.org/10.1016/j.jpowsour.2014.01.060

$$\text{Cathode}: \ VO^{2+} + H_2O \leftrightarrow VO_2^+ + e^- + 2H^+ \quad E^o = 1.00\,V \text{ vs. RHE} \tag{2}$$

Bipolar plates are one of the main components of VRFB. They should possess high electrical conductivity, good mechanical stability, corrosion resistance and electrochemical durability in the electrolyte [4]. Polymer based conductive composites are promising materials for the production of bipolar plates. Due to their structural stability against acidic medium of the electrolyte, they do not demand protective layer deposition unlike metallic bipolar plates. Polymeric composites are produced in relatively short cycle times by processes like injection molding and machining of proper final structures costs less time and capital compared to carbon–carbon composites. As polymer matrix itself is an insulator, the main afford is given to increase the electrical conductivity of composites by addition of conductive fillers such as graphite [5] carbon fiber [6], carbon black [7] and carbon nanotubes [6]. Dispersion and distribution of fillers, their aspect ratio, purity and the interaction between filler and polymer matrix are crucial to have high electrical conductivity and good mechanical properties. Carbon fibers and carbon nanotubes have lower percolation thresholds due to their high aspect ratios however graphite and carbon black filled polymers need more filler to achieve certain electrical conductivities [6]. Fillers like carbon nanotubes tend to agglomerate due to their van der Waals forces between individual particles therefore, to benefit from their unique properties, they must be well-dispersed inside the polymer. This may be achieved by optimizing process parameters of compounding [8] or using suitable additives to increase the interaction between the filler and the polymer [9].

In this study, polyphenylene sulfide was selected as the matrix material due to its higher stability in acidic medium and possibility to be used in high-temperature applications. Synthetic graphite was the main filler with spherical particle shape to obtain isotropic electrical properties. Carbon nanotubes were chosen as secondary filler to act as bridge between graphite particles to improve especially electrical conductivity of bipolar plates. Titanate based monoalkoxy coupling agent was used to decrease the overall viscosity of the composites to ensure the breakage of CNT agglomerates and to facilitate the processing of mixture both in extruder and injection molding.

2. Experimental

2.1. Materials

Polyphenylene sulfide (PPS) was Ryton V-1 grade commercial polymer from Chevron Phillips with melt flow 5000 g 10 min^{-1}. PPS was used in powder form. Synthetic graphite with low anisotropy in particle shape, KS5-75TT (d90 = 70 μm) was purchased from TIMCAL Graphite & Carbon. NC7000 grade multi-wall carbon nanotubes (average diameter = 9.5 nm, average length = 1.5 μm, 90% carbon purity) was obtained from Nanocyl, Belgium. KR-TTS, titanate-based monoalkoxy coupling agent (Titanium IV 2-propanolato, tris isooctadecanoato-*O*) was supplied from Kenrich Petrochemicals, Inc. Conventional bipolar plate from Schunk Company (FU 4369) with a thermoset binder was used as a commercial reference for the produced bipolar plates. According to the data sheet, FU4369 grade bipolar plate has in-plane electrical conductivity of 111 S cm^{-1} and through-plane electrical conductivity of 53 S cm^{-1}.

2.2. Production of bipolar plates

Polyphenylene sulfide was dry mixed with conductive fillers and coupling agent in two steps. In the first step, PPS was filled into a Papenmeier mixer and the 3 wt.% coupling agent was added by direct syringing on the dry polymer for samples S-4 to S-6. To obtain homogenous dispersion of coupling agent into PPS matrix, they were mixed during 8 min at 1000 rpm. Secondly, samples with coupling agent and the pure PPS were filled into plastic bags and the calculated amount of graphite and carbon nanotubes were added separately. The final mixture was prepared by hand-mixing. Total filler concentration was fixed to 72.5 wt.% in order to avoid the negative effects of high viscosity in injection molding. Graphite was substituted with by CNTs at different concentrations: 0, 1.25 and 2.5 wt.%. The compositions of the produced bipolar plates are given in Table 1. The prepared masterbatches were processed with Berstroff ZE 25 × 48D co-rotating twin-screw extruder with 2.5 kg h^{-1} throughput and 300 rpm screw speed. Temperature profile was: 60 °C–315 °C–320 °C, at feeding, mixing and die respectively. Granules were collected into water-bath and dried in vacuum-oven overnight. To produce bipolar plates; granules were fed into the hopper of Demag Ergotech 100/420-120 El-Exis S type injection molding machine. Plates were injected into a mold cavity with 600 mm s^{-1} injection speed and mold temperature was held at 140 °C. The temperature profile of barrel was; 345–340–340–330 °C from feeding through the die. Bipolar plates were produced in the size of 100 mm × 100 mm × 3 mm. Specimens for electrical, mechanical and electrochemical tests were prepared by laboratory scale, water-cooled saw.

Table 1
The composition of produced bipolar plates.

Samples	PPS wt.%	Graphite wt.%	CNT wt.%	Titanate wt.%
S-1	27.5	72.5	0	0
S-2	27.5	71.25	1.25	0
S-3	27.5	70	2.5	0
S-4	24.5	72.5	0	3
S-5	24.5	71.25	1.25	3
S-6	24.5	70	2.5	3

2.3. Characterization of bipolar plates

Electrical conductivity of samples was tested both in through-plane and in-plane (bulk) directions. In-plane electrical conductivity was tested according to ISO 3915 standard method. Samples were cut into 70 mm × 10 mm × 3 mm size. When current flows from one side to another, voltage drop was measured from the middle of the specimen with 1 cm electrode-span. Test setup for through-plane measurement (Fig. 1) was prepared with gold coated-copper plates (electrodes) which were protected by polyvinyl chloride (PVC) covers and samples were cut in the dimensions of 10 mm × 10 mm × 3 mm. GDL paper (35 AA) from SGL Carbon was used to decrease the contact resistance between electrodes and bipolar plates. Both in through-plane and bulk conductivity

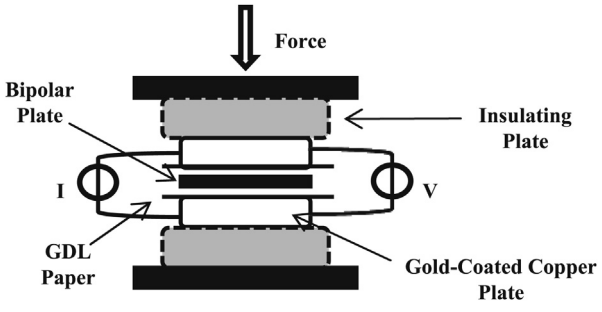

Fig. 1. Through-plane electrical conductivity setup.

measurements, current was applied by Keithley 2400 type DC power source and the voltage drop across the specimen was measured with Fluke 87 V True RMS multimeter. To maintain good contact between bipolar plate and the copper electrodes, 1 MPa pressure was applied in through-plane measurements. Polymer rich surface layer which typical for injection molded bipolar plates was removed by grinding grinded 0.1 mm from each side of the sample prior to through-plane electrical conductivity test.

Mechanical stability of bipolar plates is an important issue for the battery application and stack preparation. Poor mechanical properties may shorten the life of the battery and lead to leakage problems inside the battery. To evaluate the mechanical properties; the prepared samples were tested according to ISO 178 three-point bending test. 2 mm min^{-1} flexural test speed was applied by Universal testing machine Inspekt Table 50KN (Hegewald & Peschke, Germany). The samples with dimensions of 60 mm × 10 mm × 3 mm were conditioned at 23 °C and 50% RH for 24 h before testing. Flexural strength values as well as flexural modulus were measured.

Supra 55 VP type field emission scanning electron microscopy (FE-SEM) from company ZEISS was used to show conductive particle dispersion inside the composite. Samples were prepared with liquid nitrogen and they were examined with high resolution in-lens detector.

Rheological properties of the bipolar plates were examined by Göttfert, Rheograph 2002, Capillary Rheometer. Apparent viscosity values (Pa s) were calculated against shear rate (s^{-1}). Capillary diameter was 1 mm. International standard of ISO 11443 was used for the rheology measurement and evaluation of test results. To interpret together with rheological properties, specific energy input (SPE) value of each composite was calculated by using process parameters of twin-screw extruder and following equation:

$$SEI = (2*M_{max}*I*(n/9550))/(E*m) \quad (3)$$

where; M_{max} is the maximum torque for one screw shaft (90 N m), I is the torque (%), n is the screw speed (rpm), E is the gear drive efficiency (0.96) and m is the throughput rate (kg h^{-1}).

Melting temperature (T_m), Heat of fusion (ΔH_m), crystallization temperature (T_c), Heat of crystallization (ΔH_c) of the composites was measured by differential scanning calorimetry (DSC) analysis after injection molding. Samples were heated in nitrogen atmosphere up to 350 °C, then cooled down to 25 °C and again heated up to 350 °C by 10 °C min^{-1} temperature rate. Crystallinity of composites (X_c) was calculated with following equation:

$$\%X_c = (\Delta H_m + \Delta H_{cold})/\left(\Delta H_f\left(1 - W_f\right)\right) \quad (4)$$

Cold crystallization is an exothermic reaction and the heat of cold crystallization (ΔH_{cold}) was subtracted from heat of fusion. Heat of fusion of 100% crystalline PPS was taken from literature as 146.2 J g^{-1} [10]. W_f was defined as weight fraction of fillers.

Corrosion measurements were carried out in Avesta Corrosion cell (Bank Elektronik) with a three electrode arrangement. The bipolar plate was used as a working electrode. A platinized titan rug served as the counter electrode and a mercury sulfate electrode was the reference. For each measurement 150 ml of 2 M sulfuric acid solution was used. Sample size was 30 mm × 30 mm × 3 mm. The cyclic voltammetry (CV) measurements were carried out with a Zahner Electrochemical Workstation (IM6ex). The CVs were carried out with a scan rate of 5 mV s^{-1} and were cycled between − 1 V and 2 V. For the corrosion tests, all samples were preconditioned with 20 cyclic voltammograms of 50 mV s^{-1} until a relatively constant cyclic voltammogram was achieved. Subsequently the current was interrupted and the open circuit potential (OCP) was recorded for 30 min. After the pretreatment and OCP-measurement the corrosion current was monitored while the potential was changed from the measured OCP value first in the cathodic then in the anodic and back in the cathodic direction. The turning point of the potential in the cathodic or the anodic direction was when the corrosion current reached 500 μA cm^{-2}.

The 3-electrode setup was prepared to test the electrochemical behavior of the bipolar plates before the cell-tests. The aim was to define the width of the potential window in which the plates can be operated and to check if they possess any side reactions in the vanadium redox flow battery medium. In this case, the bipolar plates were both working and counter electrodes while mercury/mercury sulfate was the reference electrode. Potentiostatic cyclic voltammetry studies were performed in a certain potential window. For V^{2+}/V^{3+} side the electrolyte of 1.6 M $V_2(SO_4)_3$ in 2 M H_2SO_4/0.05 M H_3PO_4 and for V^{4+}/V^{5+} side electrolyte of 1.6 M $VOSO_4$ in 2 M H_2SO_4/0.05 M H_3PO_4 were used. Each sample was tested at different scan rates (20–40–60–80–100 mV s^{-1}). Diffusion coefficient (cm^2 s^{-1}) and heterogeneous rate constant (cm s^{-1}) were calculated for V^{4+}/V^{5+} side by using derivatives of Randles–Sevcik equation from the literature [11].

A single vanadium redox flow test-cell was constructed for the evaluation of the produced bipolar plates in real-battery medium [12]. Samples were prepared in the dimensions of 85 mm × 60 mm × 3 mm and with 40 cm^2 active area. For galvanostatic charge–discharge test, constant current was applied from 1 to 4 Ampere (A) by BaSyTec battery test software, obtained voltage was controlled within 0.8 V and 1.6 V and discharge power densities (mW cm^{-2}) as well as energy efficiency were calculated.

3. Results and discussions

3.1. Electrical conductivity measurements

Through-plane electrical conductivity (Fig. 2) is the measure of electron transfers in the same direction of electron flow inside the battery. However, in-plane (bulk) electrical conductivity is widely published and considered as standard threshold for bipolar plate production. The electrical conductivity increases in both directions by substitution of graphite with CNTs and by addition of the coupling agent. Samples from S-1 to S-3 prove the positive contribution of CNTs to the electrical conductivity of highly filled matrices. CNTs act as bridges between graphite particles due to their high aspect ratio [13]. This phenomenon was also visualized by FE-SEM pictures of cryo-fractured samples. CNTs are seen as

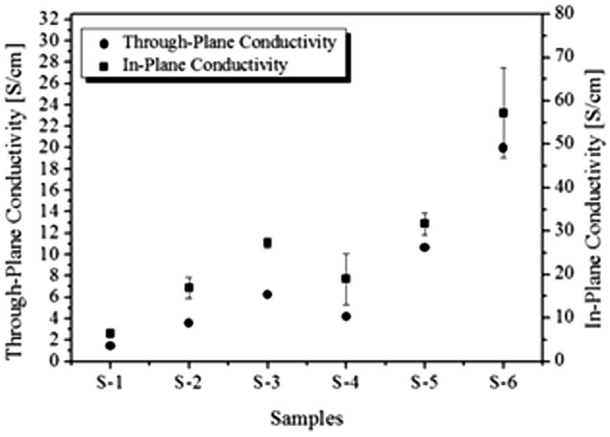

Fig. 2. Effect of CNT and coupling agent concentrations on through-plane and in-plane electrical conductivities.

dispersed in polymer matrix which fills the gap between graphite particles. It is also observed that graphite particle size decreased during processing (Fig. 3a and b).

CNTs decrease the inter-particle resistance between the main fillers. The relatively low anisotropic behavior obtained in the electrical conductivity measurements can be attributed to the low-anisotropy of the chosen graphite particles. The main challenge of using CNTs is the necessity of breaking up their agglomerates; otherwise it is hard to benefit from their unique electrical properties [14]. To overcome this obstacle, titanate-based coupling agent, KR-TTS was used. This additive was responsible of decreasing the viscosity of the composite in order to be able to process it easily in the twin-screw extruder and injection molding machine while giving a chance for better wetting of the conductive fillers by the polymer. In parallel to this effect, the decreased overall viscosity helped the dispersion of fillers, especially CNTs, more uniformly inside the matrix. As a result of this, in-plane and through-plane electrical conductivities of the composite S-6 reached up to 70 S cm^{-1} and 20 S cm^{-1} respectively. These values are almost 3 times higher compared to the sample S-3 which has the same conductive filler amount but no titanate coupling agent.

3.2. Flexural strength test

The dispersion of CNT agglomerate is also an important approach to improve mechanical properties of bipolar plates. CNTs were chosen because of their individually very high mechanical strength properties [14] but if they are not well-dispersed inside the polymer matrix, this may decreases the flexural strength values. When mechanical stress is applied during the measurement, if good interaction between CNTs and polymer is not established, agglomerates may act as stress-concentrations which makes the material more brittle [15]. Composites without coupling agent (S-1/2/3) showed that the samples with CNTs have higher flexural strength (Fig. 4) than only graphite filled-PPS. The addition of 1.25 wt.% CNT increased the flexural strength almost 15%. When more CNTs are introduced to the composite (S-3), due to the lack of enough polymers to wet CNTs, mechanical properties may start to decrease. The lower flexural strength of samples with the coupling agent can be explained by the decreased concentration of PPS which was substituted by KR-TTS and that could counterbalance the positive effect of CNTs on the mechanical properties of the samples. If the minimum requirement of flexural strength value for polymer composite bipolar plates (25 MPa) [13] is considered; all produced plates are highly above this threshold.

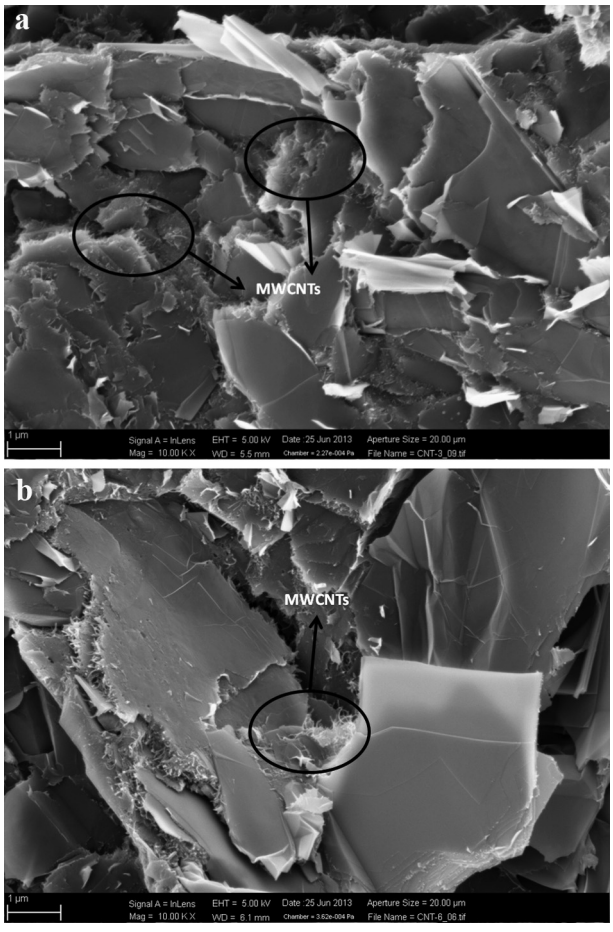

Fig. 3. a) and b) FE-SEM pictures of cryo-fractured S-6 sample.

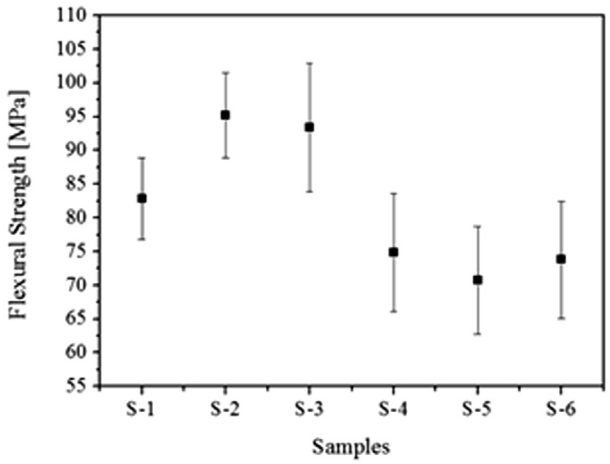

Fig. 4. Effect of CNT and coupling agent addition on flexural strength of bipolar plates.

Flexural modulus (Table 2) can be used to compare the brittleness of the composite materials. The higher the modulus value, the more brittle is the sample. The flexural modulus values of bipolar plates with the titanate additive are lower compared to their counter samples without the additive. Similar to the case of flexural strength, decreased polymer amount could be the reason for this. On the other hand the titanate based additive could also cause softening of the rather brittle PPS polymer.

3.3. Capillary rheometer analysis

The addition of carbon based fillers into polymer matrix has different effects on the resistance of composites against melt flow. This effect varies with filler shape, size and concentration [16]. The rheological behavior of the produced composites was examined by capillary rheometer (Fig. 5) in a defined shear rate window. Composites with/without carbon nanotubes and coupling agent showed

Table 2
Flexural modulus of bipolar plates.

Samples	Flexural modulus [MPa]	St. dev.
S-1	32,887	4163
S-2	38,077	4141
S-3	35,052	3464
S-4	30,463	1446
S-5	29,545	2027
S-6	27,871	881

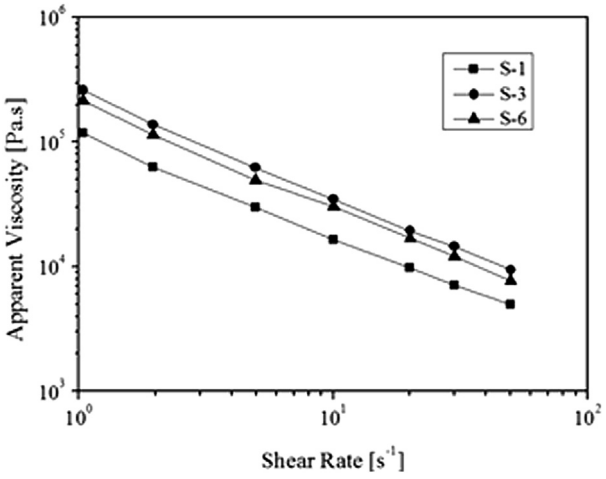

Fig. 5. Effect of CNT and coupling agent addition on apparent viscosity of produced composites.

non-Newtonian behavior. Carbon nanotube filled sample (S-3) had an almost 2 times increase in apparent viscosity compared to the sample without CNTs (S-1). Higher surface area of CNTs gives a chance for more filler–polymer interaction which increases the composite viscosity. Beside increased viscosity, chemically or physically developed filler matrix interaction is another sign for higher viscosity values and Lafdi et al. showed that such an interaction is also beneficial for mechanical properties [17]. In this perspective, capillary rheometer results correlate well with flexural strength values for the samples S-1 and S-3.

Apparent viscosity results showed that the contribution of titanate based coupling agent to composites was more like a lubricant effect than coupling of fillers and polymer matrix. By addition of coupling agent to sample S-3, apparent viscosity decreased (S-6). This result also correlates well with specific energy inputs of extruder (Table 3). The addition of coupling agent facilitated the flow of the composite in the extruder and lower torque values were obtained. As it was already mentioned before that bonding or linking of filler and polymer should exhibit higher viscosity values due to hindered behavior of polymer chains [18]. In our case, titanate based additive may have decreased the friction between filler–filler and filler–polymer system which makes the flow of composite easier.

3.4. Differential scanning calorimeter analysis

Differential scanning calorimeter analysis (Table 4) was performed to study the effects of the coupling agent and carbon nanotubes on thermal behavior and crystallinity of the produced composite materials. Melting temperature (T_m), crystallinity (X_c), heat of cold crystallization (ΔH_{cold}) and heat of fusion (ΔH_m) were calculated from the second heating curve. Heat of crystallization (ΔH_c) and crystallization temperature (T_c) data were obtained from

Table 3
SEI values of PPS based composites.

Samples	Torque (%)	SEI (kWh kg^{-1})
S-1	15	0.35
S-2	14	0.32
S-3	16	0.37
S-4	7.5	0.17
S-5	7	0.16
S-6	7	0.16

Table 4
DSC analysis results of pure PPS and produced composites.

SAMPLES	T_m (°C)	ΔH_m (J g^{-1})	ΔH_{cold} (J g^{-1})	T_c (°C)	ΔH_c (J g^{-1})	X_c (%)
Pure-PPS	282.01	43.70	17.81	218.60	49.91	42.07
S-1	283.96	8.15	9.39	251.19	13.66	43.61
S-2	283.59	9.40	4.72	251.02	15.01	35.10
S-3	283.53	9.23	8.50	251.39	16.55	44.08
S-4	283.50	7.31	7.72	251.61	12.51	41.96
S-5	282.82	8.58	11.26	251.18	12.91	55.40
S-6	282.55	8.71	10.07	250.77	12.58	52.44

the cooling curve. All the samples with conductive fillers showed slightly higher melting temperatures than pure PPS (Table 2). This increase was between 0.5 and 2 °C. Conductive fillers like graphite and carbon nanotubes may shift melting point of composites due to their higher thermal conductivity. Those fillers control heat dissipation and retard the phase change of the polymer. Similar results were also observed by thermal gravimetric analysis (TGA) [19]. In the cooling step, the influence of fillers appears as changes in the crystallization temperatures. The produced samples have higher crystallization temperature than pure PPS. It can be also interpreted as crystallization behavior facilitated by fillers which may act as nucleating agents [20]. Neither in melting nor in crystallization temperature values, there was any clear difference among different composites. This could be the explained by the high filler content in all composites.

In the literature, it has been shown that the comparison of heat of fusion (ΔH_m) and crystallinity of composite (X_c) are useful indicators to study the interaction between the fillers and the polymer [21]. Well-established polymer filler interaction restricts the movement of polymer chains during the melting process and increases the necessary heat which should be given to the sample. As the crystallinity of composite was calculated by using heat of fusion it would be also possible to get indirect explanation about polymer–filler interaction by interpreting crystallinity results.

The slight difference in the heat of fusion of the samples without additive can be attributed to the measurement and interpolation sensitivity because their melting temperatures are also close to each other. Unexpectedly, the samples with additive didn't show any increase in the heat of fusion compared to their reference samples without additive. The reason could be the high carbon content and purity of conductive fillers that were used in this study. In the absence of functional groups like hydroxylic, carboxylic and so on, it is not favorable to obtain strong interaction between the filler and the polymer. DSC analysis is made with samples in the weight of mg. Such low amounts can bring filler and polymer concentration deviations. When small changes occur in the homogeneity of composite from specimen to specimen, this could directly affect the calorimetric behaviors. In this case, it should be also taken into account that S-4, S-5 and S-6 have 3 wt.% lower PPS content than the other samples. However, some of the samples showed higher crystallinity than pure PPS, according to abovementioned points, it would be scientifically more accurate to propose that titanate based coupling agent actually increased the filler–filler interaction which is the sign of higher electrical conductivities but didn't bring improvement to filler–polymer interaction.

3.5. Corrosion measurement and cyclic voltammetry

Corrosion measurements (Fig. 6) were performed with 3 different bipolar plates to study the effect of the carbon nanotube and the titanate coupling agent addition. The polarization curves of the samples showed that all the produced samples have similar anodic currents at higher potentials. The smooth peak of S-6

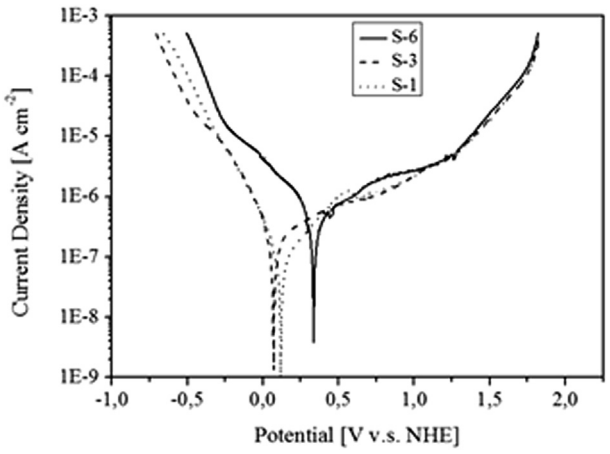

Fig. 6. Corrosion measurement of selected bipolar plates in 2 M H_2SO_4 solution with scan rate of 5 mV s^{-1}.

around 0.75 V can be the beginning of carbon corrosion and/or intercalation of sulfuric acid by-products between graphite layers which causes its oxidation [22]. The sample with the titanate coupling agent (S-6) had higher cathodic currents than the other bipolar plates. This result can be concluded as either early start of hydrogen evolution or possible reaction of H_2SO_4 solution with the titanate which could lower the corrosion resistance. Addition of carbon nanotubes (S-3) resulted in only negligible shifts of the corrosion potential to more negative side compared to graphite-based sample (S-1) and no significant difference was obtained in the anodic or cathodic currents.

As mentioned in the experimental, injection molded samples exhibit a polymer rich skin on the surface, which protects them from corrosion. Surface grinding of the samples expose the conductive fillers directly to the corrosive medium. However this step is crucial for lower contact resistances, its negative influence should be taken into account when corrosion measurement results are interpreted. The standard of Department of Energy, US requires corrosion current densities lower than 1 μA cm^{-2} [13] for the application of bipolar plates in Fuel Cells. However, this standard is not directly applicable to VRFB due to different electrolytes and operation principles.

Fig. 7 shows cyclic voltammograms of different bipolar plates. Positive and negative half-cell analyses were performed

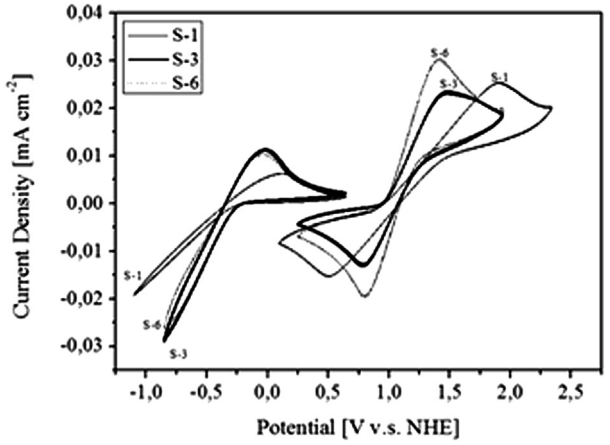

Fig. 7. Cyclic voltammograms of selected bipolar plates for the redox reactions of V^{2+}/V^{3+} and V^{4+}/V^{5+}.

independently. The peaks for oxidation and reduction reactions between V^{4+}/V^{5+} are visible at peak potentials: 1.5 V and 0.8 V for S-3, 1.4 V and 0.8 V for S-6 and 1.9 V and 0.5 V for S-1 respectively. The sample without CNTs (S-1) showed higher peak potential separation which is an indication of lower reversibility but the addition of CNTs and the titanate-coupling agent made the redox reactions more reversible. Although, the reversibility was affected positively, the peak separation potentials are over 500 mV for both S-3 and S-6 samples. In electrochemistry, some processes can be reversible at low scan rates and start to deviate through irreversibility with higher scan rates [23]. These reactions are called quasi-reversible and one of the criteria for this type of reactions is having a peak potential separation, ΔE_p:

$$\Delta E_p > 59/n \text{ (mV)} \quad (5)$$

$n = 1$, is the number of electrons transferred during redox reaction of V^{4+} and V^{5+}.

All bipolar plates can be classified as quasi-reversible for redox reaction between V^{4+} and V^{5+}. To evaluate the difference between reaction kinetics of bipolar plates, their diffusion coefficients and heterogeneous rate constants were calculated and given in Table 5.

The highest diffusion coefficients and rate constants can be found with sample S-6. Higher rate constant indicates that after a change in potential, the equilibrium between oxidation and reduction is re-established quickly. Diffusion coefficient as well as higher peak currents indicates improved redox reactions on the surface of S-6 compared to the other composites.

For the reactions of negative half-cell of the battery, oxidation peaks of V^{2+} to V^{3+} are seen at potentials around 0 V for all produced bipolar plates but the reduction peak is insignificant. The reduction of V^{3+} could be masked by the hydrogen evaluation which starts at closer potentials. According to general outcome of cyclic voltammogram, CNT-filled bipolar plates exhibit higher peak current densities. This may be attributed to their higher electrical conductivity and to the high surface area of the CNT filler.

3.6. All-vanadium redox flow battery cell-test

Laboratory scale vanadium redox flow battery test cell was prepared as explained in the "Experimental" section. 10 galvanostatic charge–discharge cycles were recorded per each current density from 25 to 100 mA cm^{-2} with an electrode area of 40 cm^2. Obtained energy efficiency and discharge power density values were presented against current densities up to 56.25 mA cm^{-2}.

The goal of the cell test was to compare the best produced bipolar plate (S-6) with commercial reference material to evaluate its potential in all-vanadium redox flow battery. Cell-tests for each material (S-6 and Schunk) were repeated 3 times with fresh bipolar plates. The results for S-6 were given separately (a, b and c) and for Schunk each data point has standard deviation even they are very low. Energy efficiency values (Fig. 8) showed that at lower current densities, carbon nanotube filled bipolar plate (S-6) shows performance as high as the commercial plate. Unfortunately, increasing current density decreases energy efficiency due to increased ohmic loss inside the battery [24]. Ohmic loss for VRFB is related to the

Table 5
Diffusion coefficient and heterogeneous rate constant of bipolar plates for the redox reaction of V^{4+}/V^{5+}.

Samples	D_o (cm^2 s^{-1})	k^0 (cm s^{-1})
S-1	2.46E-08	3.73E-04
S-3	7.92E-08	3.10E-04
S-6	9.13E-08	4.62E-04

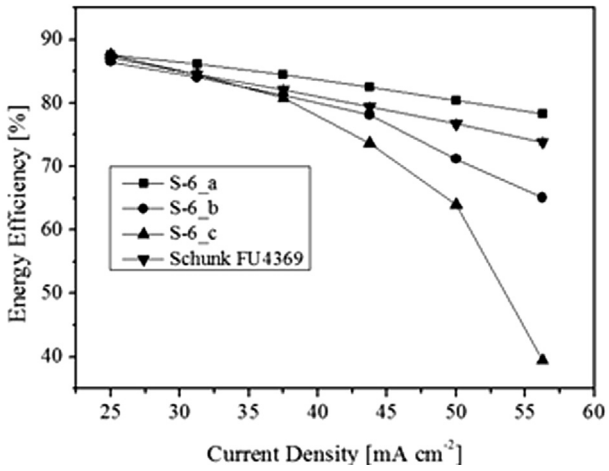

Fig. 8. The energy-efficiency vs. current density results of all-vanadium redox flow cell tests with S-6 (a, b and c) and commercial bipolar plates.

contact resistance between the graphite electrode and the bipolar plate, the individual electrical resistivity of the electrode and the bipolar plates and the ionic resistivity of the proton exchange membrane and electrolyte [25]. If it is considered that the only difference between the cells was the bipolar plate then ohmic loss can be related to intrinsic electrical resistivity of the plate and its contact resistance with the graphite electrode. It's was shown that Schunk FU 4369 bipolar plate has lower through-plane electrical resistivity than S-6 which facilitates electron transfer even at higher current densities (>50 mA cm^{-2}). Moreover, surface grinding of S-6 to remove polymer rich-layer is supposed to be helpful to decrease the contact resistance between graphite felt and bipolar but imperfect grindings could introduce surface roughness which weakens this contact and increases the resistance between these two components.

Fig. 9 shows that the vanadium redox flow test cell which was prepared with S-6 bipolar plate reaches 50 mW cm^{-2} discharge power density which can be accepted as minimum threshold value for VRFB and also possess higher discharge power densities compared to Schunk bipolar plate. Higher power density can be attributed to elevated reaction rate on the surface of electrode and also to higher discharge voltage value. However, redox reactions occur on the porous electrode surface, still small amount of those

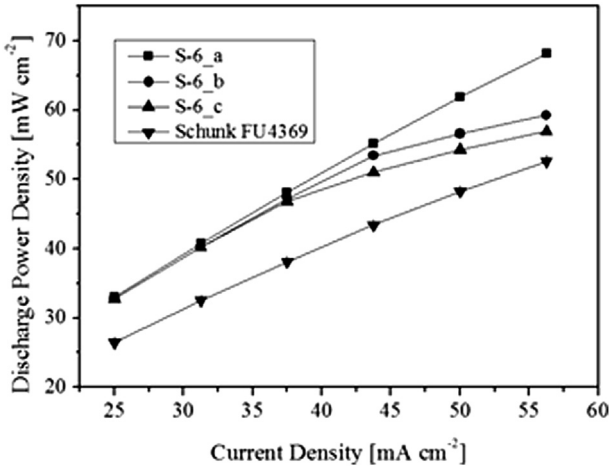

Fig. 9. The discharge power density vs. current density results of all-vanadium redox flow cell tests with S-6 (a, b and c) and commercial bipolar plates.

reactions may happen on the bipolar plate surface which was also shown by 3-electrode setup analyses. As, porous graphite electrode was the same in both setups; the difference may came from the surface properties of bipolar plates itself. Grinding of polymer layer could make the surface of S-6 bipolar plate, more favorable compared to Schunk FU 4369 to electrochemical changes. As a result, redox reactions of vanadium species may be enhanced on carbon-fillers of produced bipolar plate.

4. Conclusions

This study showed the potential of using PPS-based conductive composites as bipolar plates in all-vanadium redox flow battery. Synthetic graphite particles with lower anisotropy were chosen to minimize the filler orientation by applied shear during injection molding. Therefore the difference between through-plane and in-plane electrical conductivities of the produced composites was relatively low. Due to the high aspect ratio and higher intrinsic electrical conductivity, MWCNTs served as bridge between graphite particles and increased overall composite conductivity. To improve the dispersion of fillers and the flow behavior of the composite, monoalkoxy titanate-based coupling agent was used. Produced composites, besides their high electrical conductivities and good mechanical stability, also gave a way to the development of bipolar plates with lower filler ratios and with bigger dimensions due to effectiveness of CNT and improved composite melt flow behavior respectively.

Unfortunately, there is no standard for the corrosion current density threshold of the bipolar plates in VRFB. Tafel plot showed that produced bipolar plates can be operated between certain potentials without destructive surface reactions such as hydrogen and oxygen evolutions or the corrosion of carbon based fillers. The grinding of the polymer rich surface to reach lower contact resistance between graphite felt could have made bipolar plates relatively less protective against acidic medium and narrowed their working potential window. In 3-electrode arrangement and related cyclic voltammetry studies, higher diffusion coefficient and heterogeneous rate constant indicated favorable redox reactions of V^{4+}/V^{5+} on the surface of CNT and titanate coupling agent filled sample. Cell-performance of bipolar plates proved them as promising candidate to be used in VRFB due to high energy efficiencies at lower current densities and higher discharge power densities compared to commercial bipolar plate.

Acknowledgments

This project has received funding from the European Community's Seventh Framework Programme (FP7/2007-2013) under grant agreement no. 238363 and the scientific work was accomplished by valuable collaboration of VTT Research Centre, Finland and Justin Richards from Fraunhofer ICT, Wolfsburg.

References

[1] M. Skyllas-Kazacos, D. Kasherman, D.R. Hong, M. Kazacos, J. Power Sources 35 (1991) 399–404.
[2] F. Rahman, M. Skyllas-Kazacos, J. Power Sources 189 (2009) 1212–1219.
[3] M. Gattrell, J. Park, B. MacDougall, J. Apte, S. McCarthy, C.W. Wu, J. Electrochem. Soc. 151 (2004) A123.
[4] V. Haddadi-Asl, M. Kazacos, M. Skyllas-Kazacos, J. Appl. Polym. Sci. 57 (1995) 1455–1463.
[5] H.C. Kuan, C.C.M. Ma, K.H. Chen, S.M. Chen, J. Power Sources 134 (2004) 7–17.
[6] R.A. Antunes, M.C. de Oliveira, G. Ett, V. Ett, J. Power Sources 196 (2011) 2945–2961.
[7] R. Dweiri, J. Sahari, J. Power Sources 171 (2007) 424–432.
[8] S. Radhakrishnan, B. Ramanujam, A. Adhikari, S. Sivaram, J. Power Sources 163 (2007) 702–707.
[9] H.-P. Xu, Z.-M. Dang, M.-J. Jiang, S.-H. Yao, J. Bai, J. Mater. Chem. 18 (2007) 229.

[10] E. Maemura, M. Cakmak, J.L. White, Int. Polym. Process. 2 (1988) 79–85.
[11] E. Sum, M. Skyllas-Kazacos, J. Power Sources 15 (1985) 179–190.
[12] J. Noack, J. Tuebke, ECS Trans. 25 (2010) 235–245.
[13] S. Liao, et al., J. Power Sources 185 (2008) 1225–1232.
[14] P.-C. Ma, N.A. Siddiqui, G. Marom, J.-K. Kim, Compos. Part A 41 (2010) 1345–1367.
[15] W. Wang, P. Ciselli, E. Kuznetsov, T. Peijs, A. Barber, Philos. Trans. R. Soc. A 366 (2008) 1613–1626.
[16] J.A. King, M.D. Via, J.M. Keith, F.A. Morrison, J. Compos. Mater. 43 (2009) 3073–3089.
[17] K. Lafdi, W. Fox, M. Matzek, E. Yildiz, J. Nanomater. 2008 (2008) 1–8.
[18] R. Yeetsorn, Development of Electrically Conductive Thermoplastic Composites for Bipolar Plate Application in Polymer Electrolyte Membrane Fuel Cell (Ph.D. thesis), Waterloo, Ontario, Canada, 2010.
[19] A. Chatterjee, B.L. Deopura, J. Appl. Polym. Sci. 100 (2006) 3574–3578.
[20] J. Sheng-Ling, G. Xiao-Yu, Z. Zhi-Yuan, J. Appl. Polym. Sci. 127 (2013) 224–229.
[21] J.E. Spruiell, Chris J. Janke, A Review of the Measurement and Development of Crystallinity and its Relation to Properties in Neat Poly(Phenylene Sulfide) and its Fiber Reinforced Composites, 2004. Oak Ridge, Tennessee.
[22] H. Liu, Q. Xu, C. Yan, Electrochem. Commun. 28 (2013) 58–62.
[23] P. Zanello, Inorganic Electrochemistry: Theory, Practice and Applications, Inorganic Electrochemistry: Chapter-2, Cyclic Voltammetry, Theory, Practice and Applications, Royal Society of Chemistry, Cambridge, 2003.
[24] B. Sun, M. Skyllas-Kazacos, Electrochim. Acta 37 (1992) 1253–1260.
[25] P. Qian, H. Zhang, J. Chen, Y. Wen, Q. Luo, Z. Liu, D. You, B. Yi, J. Power Sources 175 (2008) 613–620.